# Real Time Simulation of Internal Faults in Synchronous Machines

A. B. Dehkordi, A. M. Gole, T. L. Maguire

**Abstract-- This paper presents the development of a real-time digital simulator model for the simulation of arbitrary internal faults in synchronous machines. The model is an extension of the embedded phase-domain model of the synchronous machine [1]. To represent a fault, the winding or windings involved in the fault are considered as a set of split windings[2,3,4,5] with their terminal nodes connected by a suitable fault impedance (or short circuit), which is switched in when the fault is applied. From the machine and winding geometry, values are calculated for the resulting set of mutually coupled inductances for this new winding arrangement.**

**The proposed method takes into account the actual geometry of the slots and the number of turns in each coil and uses an off-line procedure to obtain the magneto-motive force (MMF) distribution due to each winding for a unit injection of current. This MMF along with the air-gap geometry information is used to calculate the flux linkages, and hence the self and mutual inductances of the windings. Thus in contrast with earlier approaches, it is able to calculate the inductances of the machine when the windings are arbitrary distributed.**

**Since this model is developed for real-time digital simulator, it has the unique feature of being a tool to test the relays designed to protect the synchronous machines from internal faults.**

**Keywords: Internal fault, synchronous machine, real-time simulation, electromagnetic transient simulation, winding distribution.**

## I. Background

DETECTION of internal faults in the stator windings is one of the areas of concern for better protection of synchronous machines. An internal fault is defined as a turn-to-turn, or turn-to-frame, insulation failure. In order to design and test the proper protection to detect internal faults, it is necessary to develop a model that accurately predicts the transient behavior of the machine under internal fault conditions. Several authors have proposed different methods to solve this problem [2,3,4,5]. A major part of such works is splitting the inductances of machine and calculating the inductances of the new set of mutually coupled inductances. A new method of calculating the inductances is proposed in this paper which takes into account the actual distribution of windings and machine geometry. To simulate the machine in real time, an embedded approach [1], is used, in which the admittance matrix for the sub-network is efficiently inverted in each time-step.

The embedded phase domain machine model has been developed [1] in a real-time digital simulator, which considers the machine as a set of mutually coupled inductances with position-varying inductances..

Fig. 1 shows the configuration of embedded phase-domain machine applicable of simulating the internal faults. The windings subject to an internal fault are split into parts with a connection point available for insertion of fault branches.

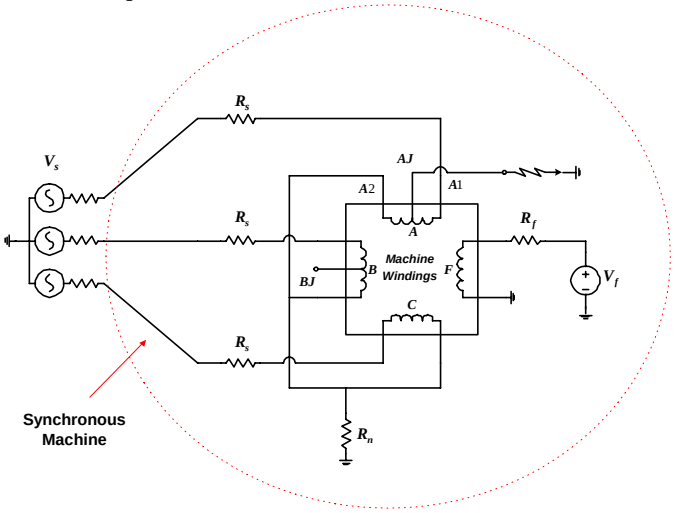


Fig. 1. Circuit diagram of embedded phase domain model of the machine, used for real-time modeling of internal faults.

In Fig. 1, the winding "A" has been divided into two parts, and now this winding has three nodes: A1, A2, and AJ. An inter-winding fault to ground can be achieved by connecting the node AJ to the circuit ground through the fault impedance. And inter-winding fault between two different phases can be done creating a similar node (i.e. BJ) inside the other winding and connect it to AJ through fault impedance.

For each connection added inside the windings, a new winding is in fact is added to the set which is mutually coupled with the other windings. Note that it is not necessary for any of these windings to be sinusoidally distributed. All

Financial support for the research was provided by RTDS® Technologies Inc and the IRC program of the Natural Sciences and Engineering Research Council (NSERC) of Canada.

A. B. Dehkordi is with the University of Manitoba, Winnipeg, Canada (e-mail: dehkordi@ee.umanitoba.ca).

A. M. Gole is with the University of Manitoba, Winnipeg, Canada (e-mail: gole@ee.umanitoba.ca).

T. L. Maguire is with RTDS Technologies Inc., Winnipeg, Canada (e-mail: tlm@rtds.com).

Presented at the International Conference on Power Systems Transients (IPST'07) in Lyon, France on June 4-7, 2007

that is required is the ability to calculate the self and mutual inductances as functions of position. This can be done in off-line calculations and before the case starts running. With the new arrangement of windings and with respect to the location of fault and rotor position all self and mutual windings must be calculated and stored. When the case is running and the position of rotor changing, these values can be read and used in the machine equations.

## II. Structure of a Synchronous Machine

This section defines the geometrical layout of a typical synchronous machine and identifies the variables that are used in the subsequent model formulation. Consider the elementary 2-pole, 3-phase wye-connected synchronous machine in Fig. 2. The stator windings of a synchronous machine are embedded in the slots around the inside circumference of the stationary member.

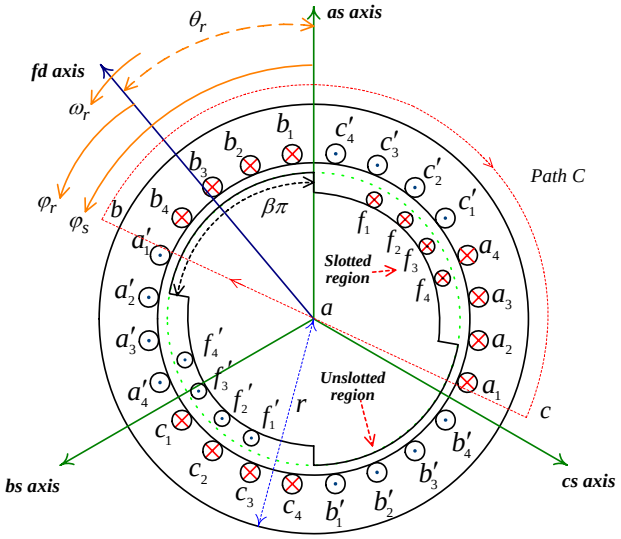


Fig. 2. An elementary 2-pole, 3-phase wye-connected salient pole synchronous machine [9].

Each phase winding of three-phase stator winding is displaced 120° with respect to the other as shown in Fig. 2. Each coil contains $n_c$ conductors in series located in two slots; one slot holds the conductors with the flow of current into the plane of the paper ($\otimes$sign) and is assigned as the positive direction. The other slot holds the conductors with the opposite flow of current ($\odot$sign). The field winding $(fd)$ is wound in the slotted region of the rotating part of the machine. Each coil on the rotor is assumed to have $n_r$ conductors. The $as, bs, cs$ and $fd$ axes indicate the positive direction of the flux produced by each of the windings.. The model also includes the damper windings, but for purposes of clarity in the explanation, they are not shown in the diagram.

The radius of the cylindrical rotor is $r$, $g_d$ is the length of air-gap in the d-axis and $g_q$ is the air-gap's length in the q-axis. $\beta\pi$ is the angle of unslotted region centered along the d-axis.

The quantities $\theta_r$ and $\omega_r$ are the angular displacement and velocity of the rotor, with $\varphi_s$ and $\varphi_r$ being the angular positions with respect to the stator $as$ axis and the $fd$ rotor axis respectively. The following equation applies:

$$\varphi_r = \varphi_s - \theta_r \tag{1}$$

## III. Procedure of Calculating Inductances

In this part a method is introduced to calculate the inductances of the above-explained machine, ignoring the saturation effect. Although explained with respect to the geometry of Fig. 2, the approach is directly applicable to other electrical machines with different geometrical structure..

### A. The Functions of Winding Distribution

Because of lack of data on winding distributions, the following example considers the case for initially sinusoidally distributed windings. This sinusoidal winding distribution has been considered earlier by others [5,7,8] and thus the results of the un-faulted case can be cross-checked against these papers. Note that even with this assumption, the faulted windings are no longer sinusoidally distributed, and so the example serves to demonstrate the validity of the proposed approach. For example, this paper shows that the results with these non-sinusoidal faulted winding are different from those calculated in the above papers as they also make the assumption that the faulted windings are also sinusoidally distributed.

With the above assumption of sinusoidal winding distributions, the winding distribution of phase winding "A" is:.

$$N_{as}(\varphi_s) = -N_s \sin(\varphi_s) \tag{2}$$

This distribution is shown in Fig. 3(a).

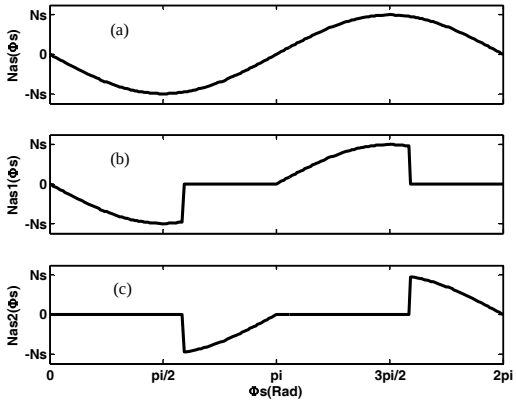


Fig. 3. (a) Sinusoidal approximation of phase "A" winding distribution. (b,c) Functions of winding distribution for sub-windings "A1" and "A2".

If the point of fault application splits the windings "A" into sub-windings "A1" and "A2", the new winding distributions for these sub-windings are shown in Fig. 3 Which are drawn with the assumption of a split at $\alpha_{brk} = \frac{7\pi}{12}$. Note that the two sub-windings have a non-sinusoidal distribution. The

windings of phases B and C can be similarly treated.

### B. The Distribution of Flux Density $(\vec{B})$

The flux density $(\vec{B})$ created by each winding can be evaluated using the Ampere's law over the "path C" located at the angular position $(\varphi_s)$ (Fig.2). If only winding "A" is energized with a current $i_{as}$, then the average radial flux density $(B_{ras})$ created by this winding "A" in each position can be expressed as:

$$B_{ras}(\varphi_s,\theta_r) = \mathrm{M}(\varphi_r) MMF_{as}(\varphi_s) \tag{3}$$

Where:

$$MMF_{as}(\varphi_s) = \int_{\varphi_s-\pi}^{\varphi_s} \left(i_{as}\cdot N_{as}(\xi)\right) d\xi \tag{4}$$

Here $\mathrm{M}(\varphi_r)$ represents the variation of the reciprocal of relative permeability of the path C due to the variation of air-gap lengths in different axes resulting from pole saliency.

The variation of $\mathrm{M}(\varphi_s-\theta_r)=\mathrm{M}(\varphi_r)$ is shown in Fig. 4, assuming a salient rotor with two different air-gap widths as in Fig. 2. The variables $\gamma_d$ and $\gamma_q$ indicated in Fig.4 are:

$$\gamma_d = \frac{1}{2\left(\frac{g_d}{\mu_0}+\frac{r}{\mu_r}\right)} \tag{5}$$

And:

$$\gamma_q = \frac{1}{2\left(\frac{g_q}{\mu_0}+\frac{r}{\mu_r}\right)} \tag{6}$$

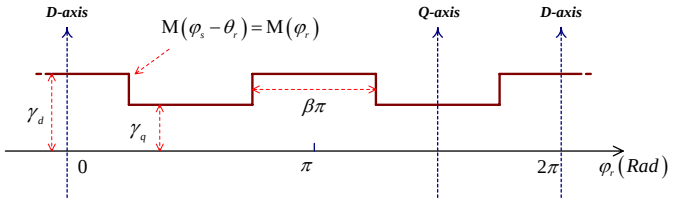


Fig. 4. Variation of function $\mathrm{M}(\varphi_r)$ with respect to angular position $(\varphi_r)$ [6].

In this paper the function $\mathrm{M}(\varphi_r)$, is assumed to be sinusoidal as defined in (7):

$$\mathrm{M}(\varphi_r) = \gamma_0 + \gamma_1\cos(2\varphi_r) \tag{7}$$

### C. Self and Mutual Inductances of the Machine With Split Windings

To calculate the self inductance and mutual inductance of a winding, it is necessary to compute the flux linking a winding due to its own current. To determine the mutual inductance the flux linking one winding due to another winding must be calculated. For this purpose let us calculate the flux linkage of a single turn of a stator winding which in this example spans $\pi$ radians and which is located at an angle $(\varphi_s)$. For example stator phase "A" induces flux on this turn that can be calculated by performing a surface integral over the surface of the single turn:

$$\Phi_{as}(\varphi_s,\theta_r) = \int_{\varphi_s}^{\varphi_s+\pi} rl\cdot B_{ras}(\xi,\theta_r)\,d\xi \tag{8}$$

Where $l$ is the axial length of the air-gap of the machine and $r$ is the radius of the inside circumference of the stator.

The flux linkage on winding "A", induced by winding "A" can be obtained by integrating $\Phi_{as}(\varphi_s,\theta_r)$ over the interval $(\varphi_s=\pi$ to $2\pi)$ considering the density of winding "A" $(N_{as}(\varphi_s))$. The interval of integration is chosen $(\varphi_s=\pi$ to $2\pi)$, because $N_{as}(\varphi_s)$ is positive in this interval.

$$\lambda'_{aa}(\theta_r) = \int_{\pi}^{2\pi} N_{as}(\varphi_s)\cdot\Phi_{as}(\varphi_s,\theta_r)\,d\varphi_s \tag{9}$$

It must be realized that some leakage flux $(L_{ls}\cdot i_{as})$ must be considered to calculate the real value of self inductance of phase "A" $(L_{aa}(\theta_r))$. The self inductance of winding "A" can be calculated by dividing the flux linkage of winding "A" by $i_{as}$:

$$L_{aa}(\theta_r) = L_{ls} + \frac{1}{i_{as}}\int_{\pi}^{2\pi} N_{as}(\varphi_s)\cdot\Phi_{as}(\varphi_s,\theta_r)\,d\varphi_s \tag{10}$$

In this paper $(L_{ls})$ is the leakage inductance derived from the manufacturer's data of the machine; however some authors proposed methods to calculate the leakage inductance from the geometrical parameters of the machine [2]. If the winding "A" is split, then similar formulations can be derived for windings "A1" and "A2". For example the self inductance of winding "A1" will be:

$$L_{a1a1}(\theta_r) = \underbrace{\frac{\int_{\pi}^{2\pi} N_{as1}(\varphi_s)\,d\varphi_s}{\int_{\pi}^{2\pi} N_{as}(\varphi_s)\,d\varphi_s}L_{ls}}_{\text{share of leakage inductance}} + \frac{1}{i_{as}}\int_{\pi}^{2\pi} N_{as1}(\varphi_s)\cdot\Phi_{as1}(\varphi_s,\theta_r)\,d\varphi_s \tag{11}$$

Please note that the leakage inductance is calculated based on the share of number of turns. Similarly the resistances of the windings are shared bases on the number of turns that each portion of winding holds.

### D. Treatment of Non-Sinusoidal Winding Distributions

The above example considered a sinusoidal distribution for the original (before fault application) windings as shown in Fig. 3(a). However, the approach is applicable to any arbitrary winding distribution by replacing the plot in Fig. 3(a) with one such as in Fig. 5 that has been drawn for a machine as in Fig. 2, considering each slot individually and assuming the same number of turns $(n_c)$ in each slot. The slots carrying current in phase "A" are indicated by; $a_1,a_2,a_3,a_4$ (current into the plane of the paper) and $a'_1,a'_2,a'_3,a'_4$ (current out of the page). This does not fundamentally change the approach as it merely substitutes a new function instead of the sinusoidal function in (2).This new function is then used in (4),(10)and (11).

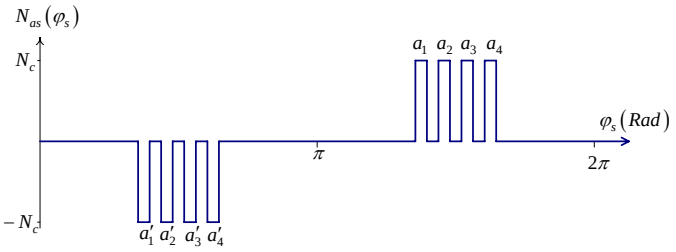


Fig. 5. The function of winding distribution for phase "A".

## IV. Parameter Estimation

Some constants such as $r, l, n_c, n_r, \gamma_0$ and $\gamma_1$ were introduced in the above section. The value of these constants is determined by number of turns in the coils, geometry of the machine and the physical properties of materials. In the absence of precise geometrical information, they can be estimated from the measured d and q axis inductances (i.e. $L_d$, $L_q$, etc.), provided by the manufactures. This calculation can be carried out off-line before commencing the time domain simulation, and hence it does not increase the on-line computation burden, which is an important consideration for real-time simulation. First the self and mutual inductances are calculated assuming starting values for the detailed parameters ($r, l, n_c, n_r, \gamma_0, \gamma_1$) with an approach as shown in (10) for the self inductance. The corresponding d-q inductances are then derived by applying the Park's transformation. These values are compared against the known d-q inductance values from manufacturer's data. Using an iterative procedure, the primary variables ($r, l, n_c, n_r, \gamma_0, \gamma_1$) can be adjusted until the correct d-q inductances are realized.

## V. Comparison with Previous Approaches and Simulation Results

This section compares the approach of this paper with that of others [5,7,8] and then shows real-time simulation results for winding faults. For comparison, the calculated inductances obtained with the proposed method are compared with those from [5,7,8]. To simulate the machine in real time, an embedded approach [1], is used. The machine's inductance matrix is converted into a corresponding admittance matrix using Dommel's trapezoidal approach [6]. The admittance matrix for the sub-network is now constructed and efficiently inverted in each time-step. As long as the calculated inductances are correct the accuracy of the simulation results performed by this embedded phase-domain model is guaranteed.

### *A. Comparison of Inductances of the Split Windings*

Consider a 100kVA, 13.8kV (L-L), 60 Hz, 2 pole, 3-phase salient pole synchronous machine which its data is shown in Table I of the Appendix. The winding inductances of this machine are calculated using the method proposed in Section III which accurately represents the distribution of the split windings, as non-sinusoidal distributions as shown in Fig. 3b and Fig. 3c. On the other hand, the method proposed in [5,7,8] approximates a sinusoidal distribution for the split windings. Such functions are in fact the fundamental space harmonics of winding distributions in Fig. 3b and Fig. 3c. The distribution of windings "A1" and "A2" using this method is shown in Fig. 6.

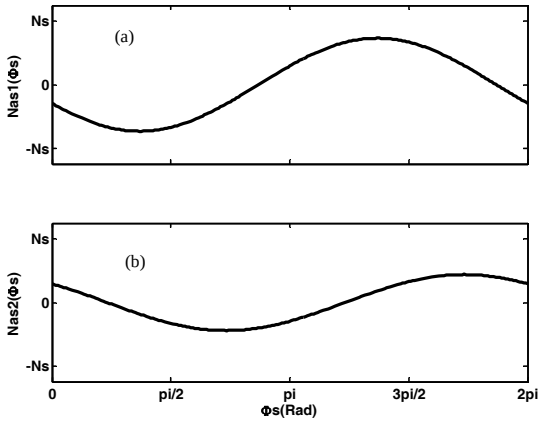


Fig. 6. Functions of winding distribution for sub-windings "A1" and "A2" assumed in method proposed in [5,7,8]. (a) Sub-winding "A1". (b) Sub-winding "A2".

Fig. 7 shows the self inductance of winding "A1" from the above mentioned two different methods, when the angular position where the winding "A" splits into two parts is $\alpha_{brk} = \frac{7\pi}{12}$.

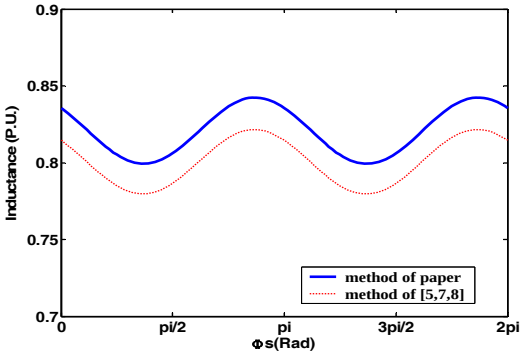


Fig. 7. Self inductance of sub-windings "A1" from the method in this paper and method of [5,7,8].

As seen in Fig. 7, the two inductances are different, particularly in their constant dc offset of about 3%. This demonstrates that the proposed approach provides different values from those with the sinusoidal assumption, but only marginally. Although not yet verified, this difference could be more prominent when the sinusoidal simplification is compared against an actual winding distribution for the original winding as shown in Fig. 5.

Fig. 8 shows the self inductance of sub-winding "A2" which is the smaller portion of winding "A" spanning an angle of $\frac{5\pi}{12}$. As can be observed when the portion of winding gets smaller, the value of self inductance will be less sensitive to the position of rotor.

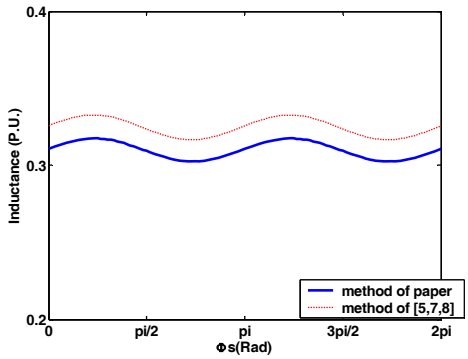


Fig. 8. Self inductance of sub-windings "A2" from the method in this paper and method of [5,7,8].

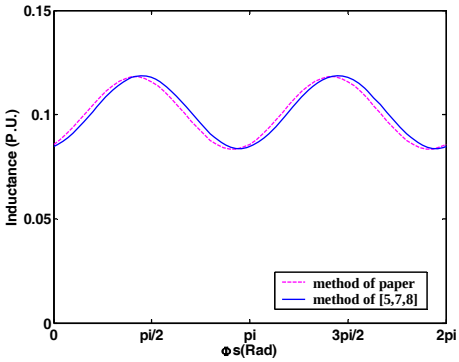


Fig. 9. Mutual inductance between sub-winding "A2" and winding "B" from the method in this paper and method of [5,7,8].

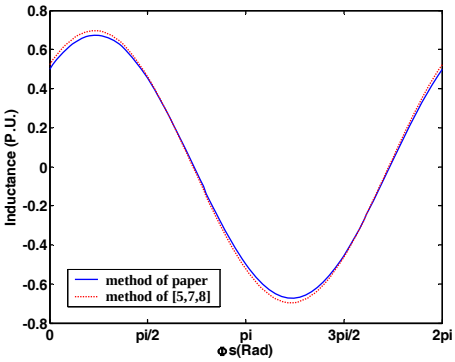


Fig. 10. Mutual inductance between sub-winding "A2" and "field" winding from the method in this paper and method of [5,7,8].

The mutual inductance between sub-winding "A2" and windings "B" and "F" are respectively shown in figures 9 and 10. The agreement between the results of these two methods is shown in figures 9 and 10 and shows a closer comparison.

### *B. Results of Simulation using Real-Time Digital Simulator*

Using the approach discussed in the opening paragraph of this section, the machine model was implemented on a real-time digital simulator from RTDS technogogies using the 3PC card which contains three Analog Devices ADSP21062 (SHARC) Digital Signal Processors (DSP). The machine model component is written in a subset of the C language available using the User Defined Code (UDC) facility available in this environment. It is expected to be a very effective tool for testing physical hardware of protection relays designed to protect synchronous machines in internal fault conditions.

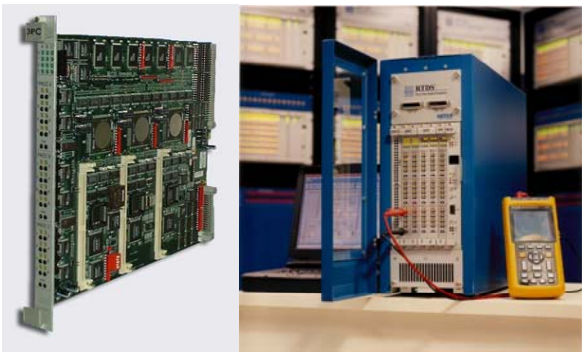

Fig. 11. 3PC card and a portable RTDS rack with n 3PC racks

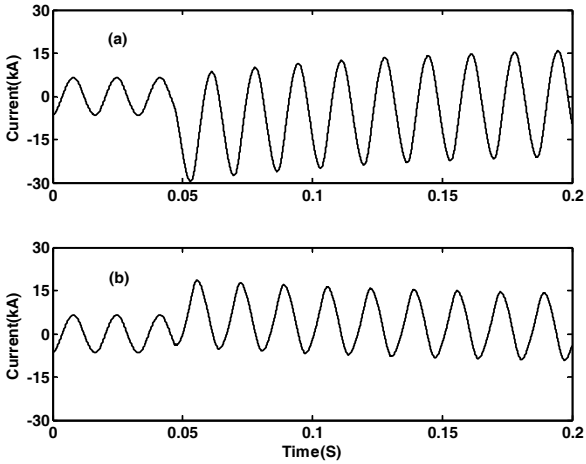


Fig. 12. Transient behavior of the machine under the internal fault condition. (a) Winding "A1" current. (b) Winding "A2" current.

Fig. 1 shows the test circuit which was used to simulate the transient behavior of the machine under the internal fault conditions. The machine is supplied by a 13.21kV (L-L), 60 Hz source. The machine is Y connected, and the neutral connection to the ground is through impedance with the resistance of $R_n = 0.19044\ \Omega$ and inductance of $L_n = 0.35364$ mH. The initial rotor angle of the machine is $\theta_0 = -60$ deg, with the machine running at rated speed. A fault to ground is applied at $0.05\ (\text{sec})$ into the simulation, from an internal point in the winding at $\alpha_{brk} = \frac{7\pi}{12}$.

As expected, before the fault the two sub-windings carry the same current equal to the steady state armature current. After the fault, the currents in the sub-windings diverge due to the changed structure of the machine.

## VI. Conclusion

A new method was presented in this paper to calculate the inductances of the machine when the windings are split. The method is based on considering the distribution of MMF in the stator space from the actual distribution of windings. An advantage of this method is that, it can also consider the actual

shape of the rotor and air-gap in calculating the inductances.

The paper also compares the inductance calculation approach of this paper to previous approaches that assume sinusoidal winding distributions for the faulted windings. The results show that the proposed method, which is based on fewer approximations, does indeed show different values for the inductances, although they are relatively small. A much larger difference could arise when the original distribution is non-sinusoidal.

The proposed algorithm was successfully implemented in real-time. Since the developed model is integrated in a real-time digital simulator, it is expected to be a very effective tool for testing the physical hardware of protection relays designed to protect synchronous machines in internal fault conditions.

## VII. Appendix

### *A. Machine data*

TABLE I
MACHINE DATA [8]

| Parameter | Symbol | Typical value |
|---|---|---|
| Line-line rated voltage | $V_{ll}$ | 13.80 kV |
| Rated power | $P_{rated}$ | 100.0 MVA |
| D-axis inductance | $L_d$ | 2.039 PU |
| Q-axis inductance | $L_q$ | 1.944 PU |
| Zero sequence inductance | $L_0$ | 0.096 PU |
| Stator leakage inductance | $l_s$ | 0.128 PU |
| Field leakage inductance | $l_f$ | 0.093 PU |
| Stator resistance | $R_s$ | 0.004 PU |
| Field resistance | $R_f$ | 0.000946 PU |

## VIII. Acknowledgment

The authors gratefully acknowledge the support of RTDS Technologies and the Natural Sciences and Engineering Research Council (NSERC) of Canada.

## IX. References

[1] A.B. Dehkordi, A.M Gole, and T.L. Maguire, " Permanent Magnet Synchronous Machine Model for Real- Time Simulation", *International Power System Transient Conference (IPST 2005)*, Montreal, June, 2005.

[2] V.A. Kinitsky, "Inductances of a portion of the armature winding of synchronous ", *IEEE Trans. PAS*, Vol. 84, no.5, pp. 389-396, May 1965.

[3] D. Muthumuni, P.G. McLaren, E. Dirks, V. Pathirana, "A synchronous machine model to analyze internal faults," *IEEE Conference on the Industry Applications*, vol. 3, pp. 1595-1600, 30 Sept.-4 Oct. 2000.

[4] A.I. Megahed, O.P. Malik, "Synchronous generator internal fault computation and experimental verification" *IEE Proceedings on Generation, Transmission and Distribution*, Vol. 145, no. 5, pp. 604 – 610, Sept. 1998.

[5] P. P. Reichmeider, D. Querrey, C. A. Gross, D. Novosel, and S. Salon, " Internal Faults in Synchronous Machines Part II: Model Performance," *IEEE Trans. Energy Conversion*, Vol. 15, no.4, pp. 372-375, Dec 2000.

[6] H.W. Dommel, "Digital computer solution of electromagnetic transients in single and multiphase networks, " *IEEE Trans. Power Apparatus and Systems"*, vol. PAS-88, no. 4, pp. 388-399, April 1969.

[7] P. P. Reichmeider, D. Querrey, C. A. Gross, D. Novosel, and S. Salon, "Partitioning of Synchronous Machine Windings for Internal Fault Analysis," *IEEE Trans. Energy Conversion*, Vol. 15, no.4, pp. 372-375, Dec 2000.

[8] P. P. Reichmeider, D. Querrey, C. A. Gross, D. Novosel, and S. Salon, "Internal Faults in Synchronous Machines Part I: The Machine Model," *IEEE Trans. Energy Conversion*, Vol. 15, no.4, pp. 376-379, Dec 2000.

[9] P.C. Krause, O. Wasynczuk, S.D. Sudhoff, Analysis of electric machinery, New York, IEEE Press, 1995.

## X. Biographies

**A. B. Dehkordi** (M'04) was born in Shahrekord, Iran. He received his B.Sc. and M.Sc. degrees in Electrical Engineering from Sharif University of Technology, Tehran, Iran in 1999 and 2002 respectively. He worked as a research engineer for Sharif University of Technology in power quality projects in 2002. He is currently a Ph.D. candidate at the Department of Electrical and Computer Engineering at the University of Manitoba. His research is on the modeling of electric machines for the Real Time Digital Simulation.

**A. M. Gole (**M'82, SM'04**)** obtained the B.Tech. (EE) degree from IIT Bombay, India in 1978 and the Ph.D. degree from the University of Manitoba, Canada in 1982. He is currently a Professor of Electrical and Computer Engineering at the University of Manitoba. Dr. Gole's research interests include the utility applications of power electronics and power systems transient simulation. As an original member of the design team, he has made important contributions to the PSCAD/EMTDC simulation program. Dr. Gole is active on several working groups of CIGRE and IEEE and is a Registered Professional Engineer in the Province of Manitoba.

**T. L. Maguire** (M'84, SM'04) was born in Canada. He graduated from the University of Manitoba with B.Sc.EE, M.Sc.EE and Ph.D. degrees in 1975, 1986, and 1992 respectively. Relevant employment experience includes time with Manitoba Hydro (1975-76), Manitoba HVDC Research Centre (1986-1994), and RTDS Technologies, Inc. (1994-present). He is a founding principal of RTDS Technologies, Inc. with a special interest in real-time simulation model development and also real-time simulation digital hardware development. He participated in creating the world's first commercial real time digital power system simulator.